IPPI

Polyolefins Journal Vol. 8, No. 2 (2021)
DOI: 10.22063/poj.2021.2893.1182

ORIGINAL PAPER

Natural rubber/natural rubber reclaim nanocomposites: Role of functional nanoparticles, mixing sequences and coupling agents

Shirin Shokoohi[1*] and Ghasem Naderi[2]

[1]Chemical, Polymeric and Petrochemical Technology Development Research Division,
Research Institute of Petroleum Industry, P.O. Box 14115-143, Tehran, Iran
[2]Departmentof Elastomer Engineering, Iran Polymer and Petrochemical Institute, P.O. Box 14565-115, Tehran, Iran

Received: 20 April 2021, Accepted: 31 May 2021

ABSTRACT

Elastomer vulcanizates based on natural rubber (NR), NR reclaim (NRR) and layered silicates were compounded in an internal mixer and cured on a two-roll mill. Cure characteristics and mechanical properties of samples based on 50NR/50NRR reinforced with Cloisite 20A, Cloisite 30B and Nanolin DK1 were compared to those of conventional NR/NRR/kaolin microcomposites. Due to the light/soft nature of organoclays suppressing the friction forces, the minimum torque values decreased in the presence of organoclays, whereas the crosslink density, evidenced by the difference between the maximum and minimum torque values, increased in all samples and scorch times shortened by 37% to a minimum in the presence of Nanolin alkaline/catalytic role in the cure reaction. Fatigue resistance improved by about 10% benefiting the crack tips blunting/energy consuming hysteresis mechanisms motivated by the organoclays among which Nanolin DK1 provides the most efficient dispersion/distribution of nanolayers by faster intragallery crosslinking reactions that pushes the stacks apart. Higher states of dispersion in this sample would also promote strain-induced crystallization under deformation responsible for the improvements seen in the modulus and elongation-at-break. Two-step mixing sequence further improved the compound performance due to the dispersion state progress confirmed by X-ray diffraction and transmission electron microscopy (20% in fatigue resistance and 53% in tensile modulus). In-situ compatibilization through bis(triethoxysilylpropyl)tetrasulfide bi-functional silane coupling agent also promoted modulus and fatigue resistance. However, a prolonged scorch time was observed due to the blinded NR cure-reactive sites as well as steric hindrance of large functional groups in the presence of this coupling agent. **Polyolefins J (2021) 8: 115-122**

Keywords: NR; reclaimed NR; organoclay; mixing sequence; coupling agent.

INTRODUCTION

Natural rubber is of great importance for many industrial and household applications. Heavy-duty tires, essential components of vibration isolation structures against earthquakes [1] and medical products such as surgical gloves in thin film forms are also based on this elastomer. Anyhow, this increasing use of rubbers in various applications has resulted in a growing volume of rubber wastes, especially in the automobile industry.

Rubbers encompassing crosslinked network structures are classified as thermoset materials which are rarely degraded; on the other hand, increasing environmental concerns and legislations have resulted in significant pressure to reduce, reuse or recycle various waste rubber products. Scrap rubbers are made up of rubber that does not meet processing and product specifications, leftover rubber from manufacturing activities and also

---

[*]Corresponding Author - E-mail: Shokoohish@ripi.ir

of old and defective rubber products. Scrap rubbers are waste and usually discharged. As mentioned above, the discarded scrap rubber does not degrade rapidly enough and this causes environmental pollutions. To reduce the pollution, there is a need to recycle scrap rubbers through devulcanization or reclaiming. Reclaiming causes the fracture of long polymer molecules and this produces rubber with lower molecular weight and tensile strength as well as broad molecular weight distribution [2], while devulcanization involves the fracture of crosslinks in the vulcanized rubber. Reclaiming, widely used in tire production, allows the conversion of vulcanized rubber into new rubber compounds that can be re-compounded into virgin polymers and then re-crosslinked. Although mechanical properties of vulcanized reclaimed rubbers are poorer those that of original rubber; improved processing, uniformity, lower heat development, thermo-plasticity, swelling, shrinkage, fast curing, good shape retention and tacking behavior as well as production costs are obtained when compounded with suitable rubbers. Reclaimed rubber, also, has been found promising for pressure sensitive applications because its tacking performance has almost shown intact with weathering. Furthermore, the anti-aging property discovered in reclaimed rubbers (RR) eliminated the need to use conventional anti-oxidants loading in rubber formulations which protects the rubber material from thermal oxidation and aging under atmospheric conditions [3]. However, at the higher reclaim loadings, the filler involved in the reclaim seems to offset the increased plasticity. Furthermore, the scorch time and tensile properties of the blends reduced with the reclaimed loading. The reduced scorch with increased cure time indicated a lower rate of cure [2-3]. Accordingly, attempts to reinforce and improve the properties of the reclaimed/virgin rubber compounds and vulcanizates have been of interest to[4] many [5] researchers [4-6]. Gumede[2] and Zhao[7] have investigated the incorporation of 10 to 90 percent of reclaimed rubber in NR matrix and its effect on the cure behavior and mechanical properties of the final compound. The outcoming results indicated that the optimum amount of reclaimed rubber in NR is 50/50. However, hardness and tensile modulus increase with increasing in reclaim rubber composition ratio resulted in more rigid NR/RR compounds.

Thitithammawong et al. [8] investigated the curing characteristics and some mechanical properties of NR/RR/PP thermoplastic vulcanizates (TPVs) prepared through a two-step mixing regime introducing PP to pre-compounded NR/RR. NR curing rate and compound processability increased with RR composition ratio (15, 30, 45 and 60 phr) while curing efficiency, dispersed particle size and tensile strength slightly decreased. A significant decrease was also observed in ultimate elongation values. Characterization of LLDPE/reclaim rubber TPVs in the presence of graphene nanoplatelets (GnPs) conducted by Paran et al. [9] revealed particle size reduction, higher thermal stability and Young's modulus besides the nucleating agent role of nanoparticles. In another research, single-walled carbon nanotubes (SWCNTs) were introduced to RR/NR compounds where RR was the dominant component with 50, 60 and 70 phr contribution in composition. Except a slight decrease in elongation-at-break, cure rate, scorch time, tensile strength and modulus increased [2].

To our knowledge, no studies have been published investigating NR reclaim/NR blends reinforced with nanoclays. Also, effect of mixing regime and in-situ contribution of coupling agents have been rarely published. In this study, effect of different layered nanosilicates including nanolin DK1, Cloisite 30B and Cloisite 20A on the physical and mechanical properties of reclaimed NR nanocomposites such as hardness, fatigue resistance, tensile modulus, elongation-at-break and rebound resilience has been compared to those of conventional kaolin microcomposites. Furthermore, effect of two different mixing sequences including simultaneous mixing and two-step masterbatch mixing was discussed on the compound properties. Effect of two different coupling agents (including TAC and Si69) was also studied.

EXPERIMENTAL

Materials

Details about materials involved in this study including reclaim rubber, natural rubber, nanoclays, kaolin and the curing package are available in Table 1.

Table 1. Materials and the suppliers.

Material	Supplier
Scrap rubber	Yazd reclaim, Iran
Natural rubber (Grade: SMR20)	Malaysia
Clay (Grade: Cloisite 30B, d_{001}=18.5Å)	Southern Clay Products, America
Clay (Grade: Cloisite 20A, d_{001}=24.2Å)	Southern Clay Products, America
Clay (Grade: Nanolin DK1, d_{001}=21Å)	Zhejiang FH Nanoclay Chem. Tech. Co., China
Kaolin	Khorasan Kaolin Co., Iran
Zinc oxide (activator, 3.5 phr)	Bayer, Germany
Stearic acid (0.5 phr)	Bayer, Germany
N-Isopropyl-*N′*-phenyl-1,4-phenylenediamine (IPPD, antioxidant, 1 phr)	Bayer, Germany
2,2'-Dithiobis(Benzothiazole) (MBTS, accelerator, 1.3 phr)	Bayer, Germany
Tetramethylthiuram disulfide (TMTD, secondary accelerator, 0.2 phr)	Bayer, Germany
Sulphur (crosslinking agent, 0.9 phr)	Bayer, Germany

Cloisite® nanoclays are produced by an ion-exchange reaction, where quaternary ammonium cations replace the sodium cations on a montmorillonite (MMT) clay surface and cationic exchange capacity (CEC) is a property of layered silicates derived from isomorphous substitution in a crystal lattice. Cloisite® 20A has dimethyl dehydrogenated tallow ammonium as the organic modifier (CEC= 95 mequiv./100g), where Cloisite® 30B is an organophilic montmorillonite (CEC = 90 mequiv./100 g) functionalized with methyl tallow bis-2-hydroxyethyl quaternary ammonium salt. Nanolin DK1 (a C18-type nanoclay), used in the present study, is a highly purified sodium-montmorillonite nanoclay with particles of 100 nm, an average dispersed thickness of platelets around 25 nm and CEC of 110-120 mequiv./100g containing octadecyl trimethyl ammonium chloride modifier functionalities. Bis(triethoxysilylpropyl)tetrasulfide (Si69) and triallylcyanorate (TAC) silane coupling agents were provided by Jiangxi Chenguang New Materials.

Preparation

NR/NRR (50/50) nanocomposite samples shown in Table 2 were processed with banbury rotors in an electrical heating Haake internal mixer (Model HBI system 90, Germany) at 100°C and a rotor rate of 60 rpm. After a two-minute rubber mastication step, IPPD antioxidant was introduced to prevent any possible degradation. Nanoclay was then added when the mixing torque reached a plateau. After 10-13 min of mixing, the curing package (according to Table 2) was introduced on a two-roll mill (Polymix, 200L, Germany) at ambient temperature set to gap size of 1 mm. Cure rate, scorch and cure times were measured at 170°C using a Zwick 4308 rheometer. Curing was then conducted by compression molding method under a hot press (Davenport, 25t, England) at 170°C. All clay types were dried under vacuum at 70°C before use.

Samples were compounded through three different mixing regimes to investigate the effect of mixing sequence. In mixing sequence "A", all components were mixed simultaneously whereas a masterbatch of NR/nanoclay or NRR/nanoclay was prepared with similar processing conditions in the first stage of "B" and "C" mixing regimes, respectively. The third component was compounded with the masterbatch on the roll

Table 2. Detailed compositions of the prepared samples (in phr).

SampleCode*→ Contents↓	A0	A1	A2	A3	A4	A5	B2	C2	BSi1	BSi2
NR	100	50	50	50	50	50	50	50	50	50
NRR	0	50	50	50	50	50	50	50	50	50
Nanolin DK1	0	0	5	0	0	0	5	5	0	0
Cloisite 30B	0	0	0	5	0	0	0	0	5	5
Cloisite 20A	0	0	0	0	5	0	0	0	0	0
Kaolin	0	0	0	0	0	5	0	0	0	0
TAC	0	0	0	0	0	0	0	0	0	2
Si69	0	0	0	0	0	0	0	0	2	0

*The capital letters A, B and C stand for the mixing sequence.

mill, as a second step, along with the addition of other additives, mentioned above.

Two typical samples (BSi1 and BSi2) were prepared to investigate the effect of Si69 and TAC silane coupling agents (5phr) on the properties of NR nanocomposites.

Characterization

Tensile tests were carried out according to ASTM D412 using an HIWA200 tensile machine at room temperature with a cross-head speed of 500 mm/min. Hardness and fatigue values were obtained using a Frank durometer (Germany) and a Monsanto fatigue machine according to ASTM D2240 and ASTM D430, respectively. Compression set of the samples was calculated according to ASTM D395 after 72 h of the test at 25°C.

The compression set test (ASTM D395) was performed on standard cylindrical specimens (D=25±0.1 mm; t=12±0.5 mm) undergone by 24 h of compression at 25% of the sample original thickness.

Dispersion state of nanoclay in the composites was characterized by a Siemens D5000 XRD machine. The nanostructure of the clay was observed by a transmission electron microscope (JEM-2100F, JEOL) of cryogenically fractured surfaces of the samples with an accelerator voltage of 200 kV.

To evaluate the dispersion of nanoclays in the polymer matrix, XRD was performed at room temperature using an X-ray diffractometer (Philips model X’Pert) in the low angle of 2θ. The X-ray beam was a Cu K_α radiation (λ= 1.540598 A°) using a 50 kV voltage generator and a 40 mA current. The basal spacing of silicates was estimated from the position of the plane peak in the WAXD intensity profile using the Bragg’s law, $d=n\lambda/(2\sin\theta_{max})$ in which d is the intergallery distance of clay, λ is the X-ray wavelength, θ_{max} is the angle related to the maximum point of first peak, and n is the diffraction sequence (n=1) [18, 19]. Specimens for X-ray diffraction were obtained by compression-molded sheets of 2mm in thickness. The nanostructure of the clay was observed by a transmission electron microscope (TEM) (JEM-2100F, JEOL) of cryogenically microtomed (with a diamond knife at -100°C) fracture surface of the samples with a voltage accelerator of 200 kV.

RESULTS AND DISCUSSION

Rheographic characteristics of NR (sample A0), NR/NRR (SAMPLE A1), NR/NRR/nanoclay (Samples A2, A3 and A4) and NR/NRR/kaolin (SAMPLE A5) compounds are illustrated in Table 3.

The minimum torque has decreased by introduction of reclaim rubber to the pristine NR due to the low molecular weight and Mooney viscosity of the matrix compound. On the other hand, the plasticizing effect of organic modifiers in Cloisite 20A, Cloisite 30B and Nanolin DK1 [10] as well as the light/soft nature of organoclays suppressing the friction forces while compounding [2] seem to decrease the torque values of A2, A3 and A4. High M_L value recorded for A5 signifies the extent of filler aggregations expected for kaolin microparticles [11]. The difference between the maximum and minimum torque values ($\Delta M=M_H-M_L$) is indicative of crosslink density of compounds which is observed to be improved in the presence of reclaim rubber, modified nanoclay and raw kaolin mineral. The additives and sulfur left over within the reclaimed rubber might be responsible for the higher abundance of crosslinks established in the presence of reclaimed rubber [12].

The ammonium modifier salts in Cloisite 20A and Cloisite 30B are shown to involve themselves in the rubber curing reaction by forming transition metal-complexes with zinc activator and sulfur curing agent, yielding polysulfidic crosslinks [13]. Thermal dissociation of Nanolin DK1 is also confirmed at 155°C where a proton and an alkyl amine are formed, catalyzing the curing reaction [14]. Moreover, regarding to the significantly high aspect ratio of organoclays, facilitated vulcanization reaction within the intercalated organosilicate layers, especially when wider intergallery spacing is available, might also be responsible

Table 3. Cure characteristics of reinforced NR/NRR samples.

Property	M_L	M_H	ΔM	t_{s2}	t_{90}	CRI
Units→	dNm	dNm	dNm	s	s	min^{-1}
A0	27	60	33	3.5	8.2	21.3
A1	22	67	45	3.2	8.8	17.8
A2	20	70	50	2.2	7.1	20.4
A3	18	67	49	2.7	8.1	18.5
A4	17	72	55	2.5	7.7	19.2
A5	23	69	46	3	8.5	18.2

for the shorter scorch time (t_{s2}) defined as the time required for incipient cure when the premature vulcanization occurs. The minimum scorch time is occurred in A2 where the alkaline media catalyzes the cure reaction [15]. Anyhow, formation of crosslinks would be hindered when the compound viscosity is higher.

Table 4 summarizes the mechanical properties of samples A0-A5 including hardness, fatigue resistance, tensile strength, elongation-at-break, compression set and resilience. Hardness measured for sample A0 is inferior to A1 containing 50% NR reclaim. Although average molecular weight of NRR is lower due to the scission of NR chains during the reclaiming process, but the filler content in NRR is responsible for the measurement results. The highest hardness belongs to A4 which is in accordance with the highest crosslink density confirmed for this sample in the recent discussion. Fatigue resistance of the NR/NRR compounds reinforced with clay (A2, A3, A4 and A5) has been improved compared to that of sample A1; in fact, energy consuming hysteresis mechanisms and the chance of crack tips blunting increase at the presence of fillers which would improve the fatigue behavior of rubber composites [16]. Furthermore, faster intragallery curing in the presence of Nanolin DK1 might push the silicate layers apart, facilitating dispersion of clay within the rubbery matrix [14, 17]. This would be beneficial for crack propagation prohibiting mechanisms justifying the higher fatigue resistance observed in A2. Extragallery crosslinking might dominate where the catalytic effect of ammonium salts is weaker or intercalation of rubber chains into the galleries is restricted. Incorporation of clay also promotes strain-induced crystallization under deformation which is responsible for the improvements seen in the modulus and elongation-at-break. This behavior would also be attributed to the interactions established at the presence of nanoclay by the intercalation of rubber chains into the clay galleries which would inevitably restrict polymer chain mobility. Although the crosslinked gel present in the NRR might be exposed as stress concentration weak points [12].

Fillers dispersed in rubber matrixes would lead to higher heat absorption/lower energy release, yielding relatively lower rebound resilience [16].

As compared to kaolin microcomposites (A5), nanocomposites (A2, A3 and A4) show much improved properties with a maximum of 42% and 100% increase in fatigue resistance and tensile modulus, respectively. The high aspect ratio of nanosilicate layers has been known to be responsible for this improvement [18].

Regarding to the characterization results, the composition corresponding to sample A2 (i.e. 50NR/50NRR/5nanolin DK1) was typically selected for further investigations on the effect of mixing sequence and coupling agents. Effect of mixing sequence is investigated comparing the cure characteristics and mechanical properties of samples A2, B2 and C2 prepared on the basis of similar composition but different mixing regimes namely A, B and C (see Table 5). Ghari et al. [19] believed that mixing sequence of Cloisite 15A and calcium carbonate nanofillers in NR has little effect on the performance of the nanocomposite whereas changes have been detected in this study when nanofillers are selectively added to the binary matrix phases through two-step compounding regimes.

The difference between the maximum and minimum torque values for B2 and C2 is higher compared to A2, indicating higher degrees of crosslinking. This could be expected due to the facilitated intercalation of rubber chains into the clay galleries through two-step mixing. However, NR chain intercalation in B mixing sequence would be more beneficial to catalytic forma-

Table 4. Mechanical properties of NR, NR/NRR and the relevant composites.

Property→	Hardness	Fatigue	Modulus 100%	Modulus 300%	Elongation-at-break	Resilience
Units→	(Shore A)	100cycle	MPa	MPa	%	%
A0	34±2	547±10	0.77±0.05	1.43±0.03	677±11	71±3
A1	39±3	418±17	0.56±0.08	0.85±0.07	592±5	58±2
A2	45±1	595±13	0.81±0.06	1.70±0.11	572±8	42±3
A3	44±1	551±7	0.69±0.05	1.33±0.02	580±5	48±1
A4	49±2	572±9	0.75±0.04	1.55±0.05	585±9	46±3
A5	41±1	493±13	0.67±0.05	0.89±0.05	564±3	55±2

Table 5. Effect of mixing sequence and silane coupling agents on the properties of NR/NRR/Nanolin DK1.

Property→	ΔM	t_{s2}	Hardness (Shore A)	Fatigue	Modulus 100%	Modulus 300%	Elongation-at-break	Resilience
Units→	dNm	s	-	100cycle	MPa	MPa	%	%
B2	56	2	52±1	660±4	0.95±0.02	2.20±0.03	573±8	37±2
C2	52	2.5	48±2	635±9	0.85±0.02	1.57±0.04	570±5	37±3
BSi1	48	2.7	49±2	691±7	1.25±0.01	2.67±0.02	602±3	30±3
BSi2	51	2.1	46±2	685±6	1.10±0.03	2.51±0.04	586±6	33±3

tion of crosslinks. Prolonged scorch time which is C mixing regime might be due to the clay sheets trapped in NRR crosslinked gel networks. Compound hardness and fatigue resistance increased in both two-step mixing regimes compared to the simultaneous mixing of nanocomposite constituents which respectively correspond to the improved CLD and dispersion obtained for B2 and C2. Direct reinforcement of NRR with nanoclay in C3 mixing regime seems to partially compensate the lower molecular weight of this phase involved in the nanocomposite. The nanocomposite modulus has improved in the samples prepared with two-step mixing regimes. In fact, higher dispersion/distribution states of nanoclay in samples B3 and C3 would support the strain-induced crystallization and matrix/filler interaction mechanisms, leading to higher modulus performance and the inferior resilience. The decrease observed in sample C3 modulus at 300% strain might be due to the low-molecular weight of the clay-reinforced phase in this sample. It seems that the mixing regime does not have any notable effect on the elongation ratio of nanocomposites samples at break.

Two coupling agents, bis-[triethoxysylil-propyl]-tetrasulfide (Si69) and triallyl cyanorate (TAC), providing different specific functionalities were used to improve the interface characteristics of NR/NRR/Nanolin DK1 nanocomposites. Roy et al. [20] reported the positive effect of silane-modified Al_2O_3 (2phr) on the maximum rheometric torque, crosslink density, cure rate index, modulus and tensile strength of NR/nano-Al_2O_3 compounds. Improved dispersion of silica in NR vulcanizates in the presence of silane coupling agents was also reported [21].

Table 5 summarizes the cure characteristics and mechanical performance of samples BSi1 and BSi2 prepared on the basis of NR/NRR/Nanolin DK1/silane (50/50/5/5) with B two-step mixing sequence. Besides, the prolonged scorch time, the difference between maximum and minimum rheometric torque, directly proportional to CLD, has decreased in the presence of both silanes. The more affected characteristics in case of Si69 could be attributed to the bi-functional nature of this coupling agent which could establish interactions with –OH groups present on the Nanolin DK1 sheets as well as NR cure-reactive sites, reducing the progress of sulfur crosslinking reactions within the NR matrix. On the other hands, the steric hindrance of the large functional group on Si69 could also be responsible for the retarded cure initiation [20-21].

Improved modulus and fatigue resistance of samples BSi1 and BSi2 confirm the effective filler/matrix interactions established in the presence of silane coupling agents which might lead to higher states of dispersion/distribution of Nanolin DK1 within the NR matrix.

X-ray diffraction results of Nanolin DK1 powder and NR/NRR/ Nanolin DK1 (50/50/5) compounded with B two-step mixing sequence (i.e. samples B2, BSi1 and BSi2) are illustrated in Figure 1. XRD (001) peaks showed a leftward shift indicative of partial intercalation of NR chains into the nanoclay galleries [22] when compared to the initial d_{001}=21 Å of Nano-

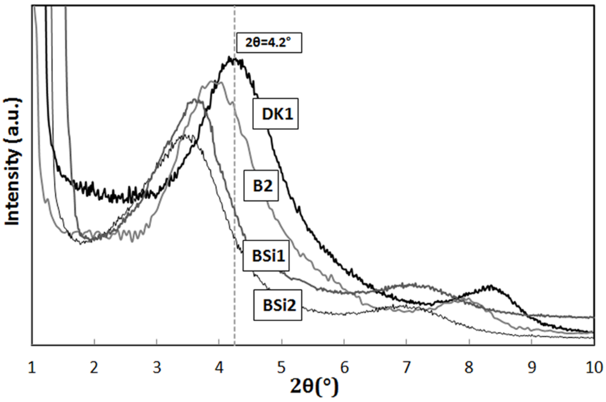

Figure 1. XRD spectrum of NR/NRR/DK1 nanocomposites: B2, BSi1 and BSi2.

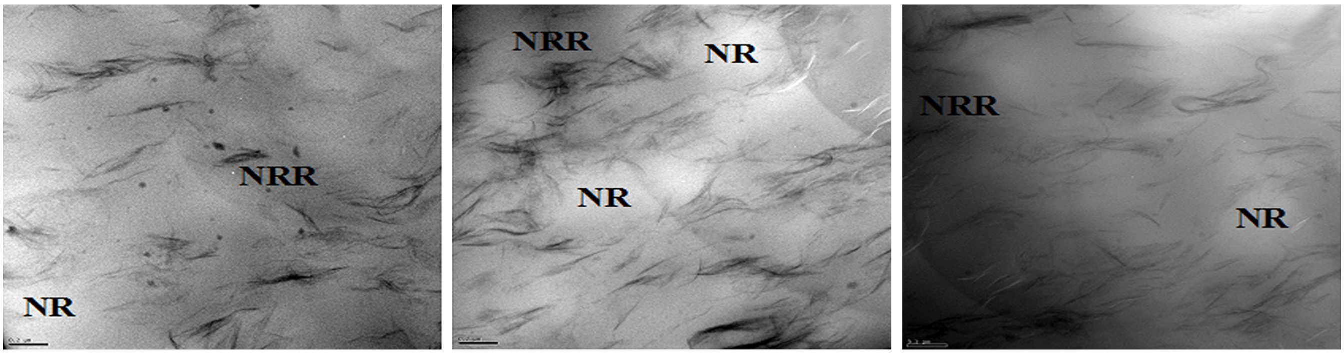

(a) (b) (c)

Figure 2. TEM micrographs of NR/NRR/DK1(50/50/5): (a) B2 (b) BSi1 and (c) BSi2 (Scale bar: 0.2µm).

lin DK1 clay powder. Sample BSi1 shows a squeezed peak with a basal spacing of 26Å confirming the results of physical and mechanical properties of corresponding nanocomposites taking the advantage of better dispersion/distribution.

TEM micrographs of samples B2, BSi1 and BSi2 confirm dispersion and delamination through partial intercalation of elastomer chains into the clay galleries suggested by the XRD results (Figure 2). Lighter areas depict the phase with lower density, i.e., NR domains and darker regions are representative of NRR phase and the rigid black lines are the transverse sections of silicate platelets. Well dispersed intercalated silicate layers were detected which is consistent with the XRD results.

CONCLUSIONS

Kaolin microfiller and three different types of nanoclay (Cloisite 15A, Cloisite 30B and Nanolin DK1) were incorporated to improve the performance of NR/reclaimed NR (50/50) compounds. Cure characteristics and mechanical behavior of reinforced vulcanizates, i.e., higher crosslink density, shorter scorch time, improved fatigue resistance, modulus and elongation-at-break, indicated that Nanolin DK1 provided the most efficient dispersion/distribution by promoting faster intragallery crosslinking reactions that pushes the stacks apart. Selected samples were prepared through different mixing sequences: simultaneous compounding of all constituents and two-step mixing regimes encompassing (NR or NRR)/clay masterbatch preparation followed by the introduction of NRR or NR in a second step. Further improvement in the modulus and fatigue resistance of samples prepared by two-step mixing regime and in-situ compatibilization through bis(triethoxysilylpropyl)tetrasulfide was also observed. In fact, NR chain intercalation in B mixing sequence seemed to be more beneficial to catalytic formation of crosslinks.

REFERENCES

1. Junkong P, Cornish K, Ikeda Y (2017) Characteristics of mechanical properties of sulphur crosslinked guayule and dandelion natural rubbers. RSC advances 7: 50739-50752
2. Gumede JI, Carson J, Hlangothi SP, Bolo LL (2020) Effect of single-walled carbon nanotubes on the cure and mechanical properties of reclaimed rubber/natural rubber blends. Mater Today Commun 23: 100852
3. Rubber S (2016) Natural rubber and reclaimed Rubber composites–A Systematic Review. Polym Sci 2: 7
4. Sombatsompop N, Kumnuantip C (2006) Comparison of physical and mechanical properties of NR/carbon black/reclaimed rubber blends vulcanized by conventional thermal and microwave irradiation methods. J Appl Polym Sci 100: 5039-5048
5. Hassan MM, Mahmoud GA, El-Nahas HH, Hegazy ESA (2007) Reinforced material from reclaimed rubber/natural rubber, using electron beam and thermal treatment. J Appl Polym Sci 104: 2569-2578
6. Sombatsompop N, Kumnuantip C (2003) Rheology, cure characteristics, physical and mechani-

cal properties of tire tread reclaimed rubber/natural rubber compounds. J Appl Polym Sci 87: 1723-1731

7. Zhao X, Hu H, Zhang D, Zhang Z, Peng S, Sun Y (2019) Curing behaviors, mechanical properties, dynamic mechanical analysis and morphologies of natural rubber vulcanizates containing reclaimed rubber. e-Polymers 19: 482-488
8. Thitithammawong A, Hayichelaeh C, Nakason W, Jehvoh N (2019) The use of reclaimed rubber from waste tires for production of dynamically cured natural rubber/reclaimed rubber/polypropylene blends: Effect of reclaimed rubber loading. J Met Mat Min 29: 98-104
9. Paran S, Naderi G, Ghoreishy M, Heydari A (2018) Enhancement of mechanical, thermal and morphological properties of compatibilized graphene reinforced dynamically vulcanized thermoplastic elastomer vulcanizates based on polyethylene and reclaimed rubber. Compos Sci Technol 161: 57-65
10. Choi D, Kader MA, Cho BH, Huh Yi, Nah C (2005) Vulcanization kinetics of nitrile rubber/layered clay nanocomposites. J Appl Polym Sci 98: 1688-1696
11. George SC, Rajan R, Aprem AS, Thomas S, Kim SS (2016) The fabrication and properties of natural rubber-clay nanocomposites. Polym Test 51: 165-173
12. Chin KP, Wan NY, Saad CSM (2011) Microcellular rubber: A study on reclaimed natural rubber (NR) latex gloves/standard malaysian rubber (SMR) 20 blends. Pertanika J Sci Technol 19: 171-176
13. Mostoni S, Milana P, Di Credico B, D'Arienzo M, Scotti R (2019) Zinc-based curing activators: new trends for reducing zinc content in rubber vulcanization process. Catalysts 9: 664-686
14. Asif A, Rao VL, Ninan K (2011) Preparation, characterization, thermo-mechanical, and barrier properties of exfoliated thermoplastic toughened epoxy clay ternary nanocomposites. Polym Adv Technol 22: 437-447
15. Dziemidkiewicz A, Maciejewska M, Pingot M (2019) Thermal analysis of halogenated rubber cured with a new cross-linking system. J Therm Anal Calorim 138: 4395-4405
16. Dong B, Zhang L, Wu Y (2017) Influences of different dimensional carbon-based nanofillers on fracture and fatigue resistance of natural rubber composites. Polym Test 63: 281-288
17. Momani B, Sen M, Endoh M, Wang X, Koga T, Winter HH (2016) Temperature dependent intercalation and self–exfoliation of clay/polymer nanocomposite. Polymer 93: 204-212
18. Bokobza L (2019) Natural rubber nanocomposites: a review. Nanomaterials 9: 12-33
19. Ghari HS, Arani AJ, Shakouri Z (2013) Mixing sequence in natural rubber containing organoclay and nano-calcium carbonate ternary hybrid nanocomposites. Rubber Chem Technol 86: 330-341
20. Roy K, Potiyaraj P (2019) Exploring the comparative effect of silane coupling agents with different functional groups on the cure, mechanical and thermal properties of nano-alumina (Al_2O_3)-based natural rubber (NR) compounds. Polym Bull 76: 883-902
21. Sarkawi SS, Dierkes WK, Noordermeer JW (2015) Morphology of silica-reinforced natural rubber: The effect of silane coupling agent. Rubber Chem Technol 88: 359-372
22. Nakhaei M, Ahmadi A, Naderi G (2020) Effect of process parameters on tensile strength of welds and modeling of laser welding of PA6/NBR/clay nanocomposite by response surface methodology. Polyolefins J 7: 99-110